Solar Phys (2015) 290:707–725
DOI 10.1007/s11207-015-0647-6

Flux Ropes as Singularities of the Vector Potential

M. Kleman[1]

Received: 25 February 2014 / Accepted: 1 January 2015 / Published online: 16 January 2015

Abstract A flux rope is a domain where a twisted magnetic field [**B**] is concentrated; it can be described as the *core* of a singularity of the outer field or the outer vector potential [**A**] (Kleman and Robbins in *Solar Phys.* **289**, 1173, 2014). This latter case, occurring when the outer field is vanishing, is mathematically analysed for a straight infinite rope. Concepts from condensed-matter physics *defect* theory are used: the flux $[\Phi]$, measured as $\oint_C \mathbf{A} \cdot \mathrm{d}\mathbf{s}$ along any loop $[C]$ surrounding the rope, is a *topological* constant of the theory. A flux rope with a small outer magnetic field can be treated as a perturbation of the above. This theoretical framework allows for the use of classical configurations inside the core, *e.g.* the linear force-free field (LFFF) Lundquist model or the nonlinear (NLFFF) Gold–Hoyle model, but restricts the number of stable solutions: they are quantised into *strata* of increasing energies (an infinite number of *strata* in the first case, only one *stratum* in the second case); each *stratum* is defined by a number $2\pi\zeta = b/r_0$, where b is the periodicity along the axis of the rope and r_0 is its radius, and the rope is made of a continuous set of stable states. We also analyse the merging of identical flux ropes (belonging to the same *stratum*), with conservation of the relative magnetic helicity: they merge into a unique rope of the first *stratum*, with a considerable release of energy.

These results might apply to ropes that nucleate in the convection zone and the photosphere, where the magnetic field outside the ropes is weak, and less accurately to the magnetic clouds (MCs) into which they evolve after coronal mass ejections (CMEs) are triggered. However, the lowest LFFF *stratum* and the unique NLFFF *stratum*, which numerically come close to each other in this analysis, match the spacecraft data remarkably well.

Keywords Flux ropes · Vector potential · Magnetic cloud models · Observations and theory · Flux rope merging

✉ M. Kleman
kleman@ipgp.fr

[1] Institut de Physique du Globe de Paris Sorbonne Paris Cité, 1 rue Jussieu, Paris cedex 05, France

1. Introduction

Magnetic fields are present everywhere on the Sun and in the heliosphere, from the bottom of the convection zone (tachocline), where they are assumed to originate, to the interplanetary space, where they expand and interact with the planetary magnetospheres. A very general feature of the configurations they adopt is in the shape of twisted flux tubes (flux ropes). The reason of this universal presence is rarely investigated; Parker (1979) long ago discussed a number of physical mechanisms to which the stability of the flux tubes might be attributed, without reaching any conclusions. In a recent review Parker (2009) still maintains the view that the fibril state of solar magnetic fields remains unexplained.

Kleman and Robbins (2014) (KR) have proposed the following explanation: We showed that a *singular irrotational (potential) magnetic field* can behave as a source for twisted flux tubes, which thus exist as *topological* objects, *i.e.* they vanish possibly when meeting singularities of an opposite sign. A flux rope is (at least) *metastable*, it carries a topological constant. This constant can be the electric current $[\mathcal{I} = (c/4\pi)\oint_C \mathbf{B}\cdot \mathrm{d}\mathbf{s}]$ or the flux $[\Phi = \oint_C \mathbf{A}\cdot \mathrm{d}\mathbf{s}]$, where C is any loop surrounding one flux rope (and only one, if other flux ropes are present). The first case ($\mathcal{I}$) was investigated by KR, the second (Φ) is the subject of the present article.

The original inspiration for the point of view developed in KR and in this article stems from the condensed-matter physics theory of *defects*. At a deeper mathematical level a full analysis of such types of electromagnetic configurations relies on the relationship between the topology of a three-dimensional domain $[\Omega]$ and the computation of divergenceless vector calculus $[\mathbf{B}]$ defined in such a domain, under the condition that $\mathbf{B}_n = 0$ on $\partial\Omega$ (tangential boundary conditions). These *harmonic knots* (so qualified because $\Delta\mathbf{B} = 0$, except on the singularities) were described in mathematical terms by Cantarella, DeTurck, and Gluck (2002) (where more general vector fields were presented as well).

In Section 1.1 we summarise the main concepts of the theory of *defects* in condensed matter physics using a very simple example. We first recognise the nature of the singularity as it originates from the divergenceless vector calculus, thus introducing the notion of *topological constant*, (see a)); then we determine that physically, a singularity must be accompanied by a *core*, (see b)). In this example the topological constant is the current. In c) we recall one of the main results derived by KR: the stable solutions are distributed over clearly distinct *strata* into each of which continuous states accumulate – each *stratum* is characterised by an energy level.

The subject to be developed in this article is introduced in Section 1.2: flux ropes whose topological constant is a flux. The magnetic field is entirely confined in the tube (no magnetic field outside) and the total current $\mathcal{I}$ through the tube vanishes (see a)). We also discuss the various situations to which the theory is applicable (see b)). In principle, one may wonder whether the theory really makes sense, since the total absence of a magnetic field outside a rope is difficult to assess. However, we show that the features characterising a flux rope vary continuously when the outer magnetic field vanishes continuously; the case with no outer field is thus an excellent approximation for the case when this outer field is small.

Section 1.3 summarises the content and main results developed in this article.

1.1. Main Concepts in the Singularity Theory of Flux Ropes

a) *The electric current as a topological constant, the* **B***-singularity.* We restrict our considerations to the most simple harmonic knot, a domain $[\Omega]$ made of the whole 3D space pierced by an infinite cylindrical hole $[\mathcal{T}]$ along the **z**-axis. According to the fundamental properties

of harmonic knots (Cantarella, DeTurck, and Gluck, 2002; KR), the irrotational field [**B**] is uniquely determined by the following:

i) boundary conditions

$$\mathbf{B}_n = 0 \quad \text{on } \partial\mathcal{T}, \qquad \mathbf{B} = \{0, 0, B_\mathrm{o}\} \quad \text{at infinity.} \tag{1}$$

We use cylindrical coordinates throughout, such that $\mathbf{B} = \{B_r, B_\theta, B_z\}$.

ii) a line integral $[\beta]$ along a closed curve $[C]$ surrounding $\mathcal{T}$ (Mahajan and Yoshida, 1998; KR)

$$\beta = \oint_C \mathbf{B} \cdot \mathrm{d}\mathbf{s}. \tag{2}$$

According to the Stokes theorem, the quantity β takes the same value if C is replaced by a homologous loop C' (**B** harmonic implies $\nabla \times \mathbf{B} = 0$). We call the constant β a *topological constant*. In the limit where the radius of $\mathcal{T}$ is reduced to a line $[L]$ (which we choose for simplicity to be along the **z**-axis), **B** becomes singular on L, and we may write

$$\nabla \times \mathbf{B} = \beta \hat{\mathbf{z}} \delta_L^2(\mathbf{r}). \tag{3}$$

B can be expressed as the gradient of a multivalued scalar field $[\psi]$, $\mathbf{B} = \boldsymbol{\nabla}\psi$

$$\psi = \frac{\beta}{2\pi}\theta + \gamma z, \qquad \mathbf{B} = \left\{0, \frac{\beta}{2\pi r}, \gamma\right\}, \tag{4}$$

where β is related to the electric current along L: $\beta = (4\pi/c)\mathcal{I}$ (*cf.* Equation (2)), $\gamma = B_\mathrm{o}$. The level sets $\psi =$ constant are ruled helicoids of pitch $-b$, with[1]

$$b = \frac{\beta}{\gamma} = \frac{4\pi}{c}\frac{\mathcal{I}}{B_\mathrm{o}}. \tag{5}$$

Thereby one can write

$$\mathbf{B} = \left\{0, \frac{B_\mathrm{o} b}{2\pi r}, B_\mathrm{o}\right\}. \tag{6}$$

These properties are reminiscent of the theory of *defects* in condensed-matter physics (Kleman and Friedel, 2008); L has the status of a vortex line endowed with a helical structure (KR) and is characterised by a scalar constant, here $[\mathcal{I}]$, akin to the circulation of a vortex line. In the example above, L is an infinite straight line, but it can be any closed loop or any curve with both ends going to infinity that carries a topological constant defined by a line integral as Equation (2), taken along any loop $[C]$ surrounding the singularity and not enclosing another singularity

$$\frac{4\pi}{c}\mathcal{I} = \oint_C \mathbf{B} \cdot \mathrm{d}\mathbf{s}. \tag{7}$$

b) *The necessity of the core*. The foregoing captures the essential topological properties of a harmonic knot, but it is of course unreasonable as a physical object because of the $1/r$

[1] A right-handed helix carries a positive pitch, a left-handed helix a negative pitch, by convention; this choice implies the use of a right-handed coordinate frame.

behaviour in Equation (6) (equivalently, the presence of a delta function in Equation (3)). This can be solved by drilling a cylindrical hole along L, thus restoring the Ω geometry; the singularity, which obeys Equation (6), is then virtual in the vacuum of the hole. Another possibility is to fill the hole with a magnetised plasma carrying an electric current $[(c/4\pi)\beta]$ – we call this region the *core* of the singularity, such that some boundary conditions (discussed below) are satisfied at the contact between this core $[\mathcal{T}]$ and the outside medium where $\mathbf{B}_\mathrm{o}$ obeys Equation (6) (from now on, we use $\mathbf{B}_\mathrm{o}$ to denote the field outside the core and $\mathbf{B}_\mathrm{i}$ the field inside the core).

This configuration provides a model for a *twisted tube* (a flux rope), insofar as the boundary conditions transmit to the core the helical nature of $\mathbf{B}_\mathrm{o}$. This can take on at least two aspects: either the magnetic field $[\mathbf{B}]$ is continuous across $\partial\mathcal{T}$, or else the magnetic field is allowed to be discontinuous (which requires a surface current for $r = r_0$). In both cases the vector potential $[\mathbf{A}]$ is continuous, *cf.* Griffiths (1999) (a discontinuity of the vector potential would imply a δ-function singularity in the $[\mathbf{B}]$-field on the boundary (see KR, footnote 2), which is most probably not physical, and is not considered).

c) *Quantised strata*. There are *restrictions* on the allowed field configurations; they have to minimise the magnetostatic energy $[\mathcal{E} = \frac{1}{8\pi}\iiint_\Omega (B_\theta^2 + B_z^2)\,\mathrm{d}V]$, under the assumption that the field 'carries' a topological constant ($\mathcal{I}$ in the case above, Equation (7)), and that the boundary conditions (continuity of $\mathbf{B}$ for $r = r_0$ or presence of a surface current; $\mathbf{B} = \{0, 0, B_\mathrm{o}\}$ at infinity) are obeyed. The calculations made in KR assumed that the field inside the flux ropes is force-free, but the core model can be chosen at will, depending on the physical characteristics of the plasma; it can be *e.g.* a linear force-free field, a uniformly twisted field (nonlinear, force-free), a non-force-free field, a field carrying a constant current density, or a linear azimuthal current.

The calculations yield critical points satisfying:

i) $\partial\mathcal{E}/\partial r_0 = 0$ (the condition of stability $\partial^2\mathcal{E}/\partial r_0^2 > 0$ has to be checked);
ii) continuity of $\mathbf{B}$ or continuity of the vector potential $\mathbf{A}$ if $\mathbf{B}$ is discontinuous (boundary conditions).

For a given electric current $\mathcal{I}$, separated sets of stable states are derived that are continuously distributed over each of these sets; the states are thus quantised into *strata*, each defined by a number $2\pi\zeta = b/r_0$, where b is the periodicity along the axis of the rope and r_0 its radius. The energies scale as $\mathcal{E} \propto b^2 f(\zeta)$. See KR and below for examples.

1.2. The Flux as a Topological Constant

a) *The* $\mathbf{A}$*-singularity.* We have dwelt on the case where the topological constant is the current; this requires that the outside field be irrotational, but non-vanishing. The assumption of irrotationality is often made, but it has also been assumed in some numerical simulations that $\mathbf{B}_\mathrm{o}$ totally vanishes, which makes simulations easier and is justified by the extremely small field measured outside the ropes, at the limit of measurement possibilities; see next paragraph. Therefore it is tempting to consider that the relevant variable is no longer the magnetic field $[\mathbf{B}]$, but the *vector potential* $[\mathbf{A}]$, $\mathbf{B} = \nabla \times \mathbf{A}$, irrotational outside the core; this is the essence of the $\mathbf{A}$*-singularity*.

In the Coulomb gauge $\nabla \cdot \mathbf{A} = 0$, $\mathbf{A}_{\mathrm{o},n} = \mathbf{A}_{\mathrm{i},n} = 0$ because of the continuity of the vector potential at a boundary (Griffiths, 1999). The magnetic field $\mathbf{B}_\mathrm{i}$ is continuous inside the tube,

outside the tube $\mathbf{B}_o = 0$. The magnetic field discontinuity at the boundary requires a surface current that compensates for the volume current inside, the total current has to vanish (KR). Within this picture the relevant *topological constant* is no longer the current $[\mathcal{I}]$, but the flux $[\Phi]$.

$$\Phi = \oint_C \mathbf{A} \cdot \mathrm{d}\mathbf{s}. \tag{8}$$

The concept of a core occupied by a flux rope is of course relevant here as in the previous case.

In the minimisation process the inner total current (equal, and opposite in sign, to the current flowing along the boundary) still plays a fundamental role. This is discussed in Section 2 in connection with the case when the outside magnetic field is smaller than the inside magnetic field and smoothly tends to zero, *i.e.*, a configuration where the topological constant, that is, the total current as long as $\mathbf{B}_o \neq 0$, suddenly turns into the other topological constant, that is, the flux, when $\mathbf{B}_o = 0$. At the same time, the field configuration changes *continuously*. This is another justification of investigating the **A**-singularity; *the domain outside a flux rope*, little magnetised as it is, *can be treated as a perturbation of the* **A**-*singularity*, *i.e.*, $\mathbf{A}_o$ *irrotational*. In other words, the **A**-singularity is an approached solution of the **B**-singularity, when $\mathbf{B}_o$ is very small. We now discuss the cases where this approximation can be employed.

b) *Confinement of the magnetic flux.* The most often cited examples of plasmas devoid of magnetic fields, except in the flux ropes, are the fluid-dominated convection zone (Fan, 2009) and the photosphere (Stenflo, 1978). The problem of emergence of a flux rope from the subphotospheric levels uses a model with neutralised currents, see *e.g.*, the review article by Hood, Archontis, and MacTaggart (2012), MacTaggart and Haynes (2014), and Török *et al.* (2014). The photospheric fibrils are also current-neutralised in most models, this question has been raised starting with the Parker–Melrose debate (Parker, 1996; Melrose, 1996), which seems to have been concluded recently in favour of Parker: currents are neutralised, except in some specific situations (Georgoulis, Titov, and Mikić, 2012).

Emerging flux ropes transform when they cross the photosphere into new flux ropes that trigger coronal mass ejections (CMEs) and are no longer current-neutralised, see *e.g.*, Patsourakos, Vourlidas, and Stenborg (2013), Schmieder, Démoulin, and Aulanier (2013), and Török *et al.* (2014). They are current-carrying singularities. They expand in the corona, where they are essentially force-free (no Lorentz force) as a result of the small plasma β-parameter and interact with the ambient magnetic field. The coronal space is thus practically filled with magnetic lines, but this does not necessarily make the description in terms of singularities useless (most probably **B**-singularities), which may be in contact along their core boundaries or separated by thin current sheets (Parker, 2004).

The example discussed at the end of this article (Section 5.3) relates to magnetic clouds (MCs) in the interplanetary space; these are the final state of the flux ropes that accompany CMEs and extend between the Sun and the Earth (Vourlidas, 2014, for a short review). Typical values extracted from the literature (*e.g.*, Möstl *et al.*, 2009) are $B_i \sim 10-30$ nT, and $B_o \sim 5$ nT. The ratio of the two quantities B_o/B_i is still high, but sufficiently lower than unity, which somewhat justifies the calculations presented in the discussion (Section 5). The obtained orders of magnitude agree better with recent spacecraft measurements: one might in fact wonder why they work so well.

1.3. Content of This Article

We investigate force-free field (FFF) models, as in KR. The Lorentz force vanishes at any point of the core; thus the Beltrami equation is

$$\ell \nabla \times \mathbf{B} = \mathbf{B}, \tag{9}$$

where ℓ is a constant on each line of force of the magnetic field, since $\nabla \cdot \mathbf{B} = 0$. The flux rope is assumed to be a circular cylinder with helical symmetry along its axis.

We explore two situations where the topological invariant is the *flux*, *i.e.*, the vector potential $[\mathbf{A}_\mathrm{o}]$ is irrotational, $\mathbf{B}_\mathrm{o} = 0$:

i) the Lundquist *linear* force-free field case (LFFF) (Lundquist, 1950), the linearity implies that ℓ is a constant over all the rope (Section 3);
ii) the Gold–Hoyle nonlinear force-free field case (NLFFF) (Gold and Hoyle, 1960), where ℓ depends on radius (Section 4).

These two **A**-singularities are continuous limits for a model where **B** is discontinuous when $B_\mathrm{o} \to 0$ (Section 2) and thus approximations of a flux rope with a small outer field.

The processes of tube merging are analysed in Sections 3 and 4. Flux ropes of the same flux sign (same sense of the magnetic axial field) belonging to any *stratum* tend to merge into a unique rope belonging to the first *stratum*, while releasing a large amount of energy, comparable to the energy of the original ropes.

In Section 5, we compare some observational data for MCs (Lepping *et al.*, 1997; Dasso, Mandrini, and Démoulin, 2003; Dasso *et al.*, 2005; Démoulin, 2014) to the theoretical results developed in Sections 2, 3, and 4. The lowest *stratum*, in the LFFF case, seems to match the observational results with a rather good accuracy, whereas all the higher *strata* do not. In the NLFFF case there is only one *stratum*, which is very similar to the LFFF lowest *stratum*. Thus it appears difficult to decide which model suits the observations better, but it is already a remarkable fact that the observations are so well fitted and that no higher *stratum* than the lowest one is observed, a result that also transpires from the theory.

2. A-Singularity as a Continuous Limit of the B-Discontinuous Singularity

In this section, it is assumed that $\mathbf{B}_\mathrm{i}$ and $\mathbf{B}_\mathrm{o}$ are discontinuous on the boundary $r = r_0$. Let B_i and B_o be their **z**-components on this boundary. According to Equation (6), $\mathbf{B}_\mathrm{o}$ can be written $\mathbf{B} = \{0, \frac{B_\mathrm{o} b_\mathrm{o}}{2\pi r}, B_\mathrm{o}\}$, where b_o is the inverse twist along the field lines outside the flux rope. The topological constant is the current $[(c/4\pi) B_\mathrm{o} b_\mathrm{o} = (c/4\pi) \oint_C \mathbf{B} \cdot \mathrm{d}\mathbf{s}]$. The limit configuration $B_\mathrm{o} = 0$, $B_\mathrm{i} =$ constant is the same as the one discussed in Section 3 below.

The only boundary condition to be satisfied is the continuity of the potential vector $\mathbf{A}_\mathrm{o}(r_0) = \mathbf{A}_\mathrm{i}(r_0)$ at $r = r_0$. The inner field configuration is helical (we are interested in flux ropes). Let b be the pitch of the inner magnetic field lines at the boundary. The expressions in Section 2.1 below show that $\mathbf{A}_\mathrm{o}(r)$ is split into an irrotational part that can be expressed, locally at least, as a gradient of helicoids of pitch b, and a part that is rotational and from which the magnetic field $\mathbf{B}_\mathrm{o}(r)$ above is derived. Note that b_o can be chosen at will regardless of b. But it will appear as a final result that the **A**-singularity is a continuous limit of the **B**-discontinuous singularity and is not related to the choice of b_o.

We restrict the calculations to the LFFF case, **A** is written in the Coulomb gauge.

2.1. Magnetic Field and Vector Potential

a) *outside*:

$$\mathbf{B}_\mathrm{o} = \left\{0, \frac{B_\mathrm{o} b_\mathrm{o}}{2\pi r}, B_\mathrm{o}\right\}, \qquad \mathbf{A}_\mathrm{o} = \left\{0, \frac{B_\mathrm{o} r}{2} + \frac{c_\theta}{r}, -\frac{B_\mathrm{o} b_\mathrm{o}}{2\pi} \ln \frac{r}{r_0} + d_z\right\}, \tag{10}$$

where c_θ and d_z are two constants determined below by the boundary conditions at $r = r_0$; these constants enter in the components of the irrotational part of $\mathbf{A}_\mathrm{o}$,

b) *inside*:

$$\mathbf{B}_\mathrm{i} = \left\{0, A J_1\left(\frac{r}{\ell}\right), A J_0\left(\frac{r}{\ell}\right)\right\}, \qquad \mathbf{A}_\mathrm{i} = \ell \left\{0, A J_1\left(\frac{r}{\ell}\right), A J_0\left(\frac{r}{\ell}\right)\right\}, \tag{11}$$

where ℓ is the length associated with the Beltrami equation. $J_0(x)$, $J_1(x)$ are Bessel functions of the first kind.

2.2. Boundary Conditions

The magnetic field is discontinuous, but the vector potential has to be continuous, as emphasised previously in the second paragraph of Section 1.1; thus

$$c_\theta = -\frac{1}{2} r_0^2 B_\mathrm{o} + r_0 \ell A J_1\left(\frac{r_0}{\ell}\right), \qquad d_z = \ell A J_0\left(\frac{r_0}{\ell}\right). \tag{12}$$

The flux inside the tube [$\Phi_\mathrm{i} = \oint_{r=r_0} \mathbf{A} \cdot \mathrm{d}\mathbf{s}$] can be calculated either with $\mathbf{A} = \mathbf{A}_\mathrm{i}$ or $\mathbf{A} = \mathbf{A}_\mathrm{o}$. This yields

$$\Phi_\mathrm{i} = 2\pi r_0 A J_1\left(\frac{r_0}{\ell}\right) = B_\mathrm{o} \pi r_0^2 + 2\pi c_\theta.$$

By definition of the helicity of the magnetic lines on the boundary, we have

$$\frac{B_{\mathrm{o},\theta}(r_0)}{B_{\mathrm{o},z}(r_0)} = \frac{b_\mathrm{o}}{2\pi r_0}, \qquad \frac{B_{\mathrm{i},\theta}(r_0)}{B_{\mathrm{i},z}(r_0)} = \frac{b}{2\pi r_0}. \tag{13}$$

Let us introduce three dimensionless parameters η, ζ_0, ζ and a magnetic field [B_i] – these parameters will soon appear as the fundamental parameters of the problem:

$$\eta = \frac{r_0}{\ell}, \qquad \zeta = \frac{b}{2\pi r_0}, \qquad \zeta_\mathrm{o} = \frac{b_\mathrm{o}}{2\pi r_0}, \qquad B_\mathrm{i} = A J_0(\eta). \tag{14}$$

With these notations, Φ_i can be written as

$$\Phi_\mathrm{i} = 2\pi r_0 \ell B_\mathrm{i} \zeta.$$

Eventually, after further use of the boundary conditions Equations (12) and (13):

$$\Phi_\mathrm{i} = B_\mathrm{i} b \ell, \qquad d_z = B_\mathrm{i} \ell, \qquad 2\pi c_\theta = B_\mathrm{i} b \ell - B_\mathrm{o} \pi r_0^2. \tag{15}$$

2.3. Electric Currents and Energies

The current inside the boundary

$$\mathcal{I}_\mathrm{i} = \frac{c}{4\pi} B_\mathrm{i} b \tag{16}$$

is given. The total current, including the current flowing along the boundary $\mathcal{I}_s = (c/4\pi)(B_\mathrm{o} b_\mathrm{o} - B_\mathrm{i} b)$, due to the **B**-discontinuity at $r = r_0$, is

$$\mathcal{I} = \frac{c}{4\pi} B_\mathrm{o} b_\mathrm{o}. \tag{17}$$

This total current is the topological constant of the model, *i.e.*, $B_\mathrm{o} b_\mathrm{o} = \oint \mathbf{B} \cdot \mathrm{d}\mathbf{s}$, when **B** circumnavigates any loop surrounding the flux rope; B_o is a given parameter (it will be made to vanish at constant B_i), thus b_o is also given, as well as B_i. When $B_\mathrm{o} = 0$, the topological constant vanishes, but another topological constant appears, the magnetic flux $\Phi_\mathrm{i} = \oint_C \mathbf{A} \cdot \mathrm{d}\mathbf{s} = B_\mathrm{i} b \ell$, where C is any loop surrounding the flux rope.

The outside $[\mathcal{E}_\mathrm{o}]$ and inside $[\mathcal{E}_\mathrm{i}]$ energies can be written as

$$\mathcal{E}_\mathrm{o} = \frac{B_\mathrm{o}^2}{4}\left(\frac{1}{2}\left(R^2 - r_0^2\right) + \left(\frac{b_\mathrm{o}}{2\pi}\right)^2 \ln\frac{R}{r_0}\right), \qquad \mathcal{E}_\mathrm{i} = \frac{B_\mathrm{i}^2}{4}\left(r_0^2 + \left(\frac{b}{2\pi}\right)^2 - \frac{b\ell}{2\pi}\right), \tag{18}$$

where R is the outer radius.

2.4. Critical Points

Let $\mathcal{E} = \mathcal{E}_\mathrm{o} + \mathcal{E}_\mathrm{i}$. The derivative $\partial\mathcal{E}/\partial r_0 = 0$ can be written as

$$\frac{\partial \mathcal{E}}{\partial r_0} = \frac{r_0}{4}\left(\left(2B_\mathrm{i}^2 - B_\mathrm{o}^2\right) + B_\mathrm{i}^2 \zeta \frac{\zeta + \zeta^{-1}}{D} - B_\mathrm{o}^2 \zeta_\mathrm{o}^2\right) = 0, \tag{19}$$

where $D = 1 - \eta(\zeta + \zeta^{-1})$. We use the same notation as in KR, where it is also proven that $\partial\ell/\partial r_0 = -(\zeta + \zeta^{-1})/D$. Assuming $D \neq 0$,

$$\left(2B_\mathrm{i}^2 - B_\mathrm{o}^2\right) + B_\mathrm{i}^2\left(1 + \zeta^2\right) - B_\mathrm{o}^2\zeta_\mathrm{o}^2 - \eta\left(\zeta + \zeta^{-1}\right)\left(2B_\mathrm{i}^2 - B_\mathrm{o}^2 - B_\mathrm{o}^2\zeta_\mathrm{o}^2\right) = 0. \tag{20}$$

There are two extreme cases and one intermediary case:

i) Continuity of $|\mathbf{B}|$. $B_\mathrm{o} = B_\mathrm{i}$. This yields $\eta = \zeta[1/(1 - \zeta_\mathrm{o}^2) + 1/(1 + \zeta^2)]$, an expression that greatly simplifies if $\mathbf{B}_\mathrm{o} = \mathbf{B}_\mathrm{i}$ (no surface current), yielding $\eta = 2\zeta/(1 - \zeta^4)$; this has been treated in KR.

ii) **A** irrotational. $B_\mathrm{o} = 0$. This yields $\eta = \zeta/2 + \zeta/(1 + \zeta^2)$, which is the same expression as that in Section 3, Equation (27); this has been treated in KR.

iii) In between, the configurations close to $B_\mathrm{o} = 0$ are the most interesting ones. Let us write

$$B_\mathrm{o}^2 = \epsilon B_\mathrm{i}^2,$$

where $\epsilon > 0$ is a small parameter. Equation (20) becomes

$$3 + \zeta^2 - \epsilon\left(1 + \zeta_\mathrm{o}^2\right) = 2\eta\left(\zeta + \zeta^{-1}\right)\left(1 - \frac{1}{2}\epsilon\left(1 + \zeta^2\right)\right). \tag{21}$$

We employ the approximations

$$\left(1-\frac{1}{2}\epsilon\left(1+\zeta_{\rm o}^2\right)\right)^{-1}\approx\left(1+\frac{1}{2}\epsilon\left(1+\zeta_{\rm o}^2\right)\right),$$

$$\left(3+\zeta_{\rm i}^2-\epsilon\left(1+\zeta_{\rm o}^2\right)\right)\left(1+\frac{1}{2}\epsilon\left(1+\zeta_{\rm o}^2\right)\right)\approx 3+\zeta^2+\frac{1}{2}\epsilon\left(1+\zeta_{\rm o}^2\right)^2,$$

and eventually, we derive

$$\eta=\frac{\zeta}{2}+\frac{\zeta}{1+\zeta^2}+\frac{\epsilon}{4}\zeta\left(1+\zeta_{\rm o}^2\right). \tag{22}$$

The configurations are continuously varying when $B_{\rm o}\to 0$. Thus the limit case $\epsilon=0$, when the vector potential is irrotational and the topological constant is the magnetic flux, describes with but a small difference a configuration $\epsilon\neq 0$ with a weak magnetic flux outside the flux rope. *Thereby a $\epsilon\neq 0$ field configuration can be studied as a perturbation of the limit configuration $\epsilon=0$, for which $\mathbf{A}_{\rm o}$ is irrotational.*

3. Linear Force-Free Field in the A-Singularity Framework

3.1. Magnetic Field and Vector Potential – Stable Critical Points

We use the results of the previous subsection with $B_{\rm o}=0$. We drop the index i of $\mathbf{B}_{\rm i}$ and of $\Phi_{\rm i}=B_{\rm i}b\ell$ because it is no longer necessary. $\mathbf{A}_{\rm o}$, which is derived from Equation (10), can now be written

$$\mathbf{A}_{\rm o}=\Phi\left(0,\frac{1}{2\pi r},\frac{1}{b}\right),$$

and satisfies the topological relationship

$$\Phi=\oint_C\mathbf{A}_{\rm o}\cdot{\rm d}\mathbf{s}.$$

Thus, the topological constant is Φ. In the previous section, the topological constant was $\mathcal{I}$, which was split into two topological constants $\mathcal{I}_{\rm i}$ and $\mathcal{I}_s$, both constant in the minimisation process. We conserve this property because of continuity, when $B_{\rm o}\to 0$. But we recall that the current has no longer a topological value, but a constant in the energy minimisation.

The results are the same as in KR (their Section 5), but presented in a simpler form. We expatiate in the next subsection on the phenomena of tube merging.

The line energy density Equation (18) can be written as

$$\mathcal{E}=\frac{B^2b^2}{16\pi^2}\left(1+\frac{1}{\zeta^2}-\frac{2\pi\ell}{b}\right)=\frac{\Phi^2}{16\pi^2}\left(\frac{1}{\ell^2}+\frac{1}{\zeta^2\ell^2}-\frac{2\pi}{\ell b}\right), \tag{23}$$

and also as

$$\mathcal{E}=-\frac{B\Phi}{8\pi}D, \tag{24}$$

because of the identities $(1/\ell^2)\{1+1/\zeta^2-2\pi\ell/b\}=(1/\ell^2\eta\zeta)\{-1+\eta(\zeta+\zeta^{-1})\}$ and $\ell^2\eta\zeta=\Phi/(2\pi B)$. We recall that $D=1-\eta(\zeta+\zeta^{-1})$.

The minimisation of the free energy, Equation (24), with respect to r_0 requires that some parameter, *e.g.*, B, b, or ℓ be fixed in addition to the topological constant Φ. As explained above, $\mathcal{I}_\mathrm{i} \propto Bb$, Equation (16), is a constant. Equivalently, since $\Phi = Bb\ell$ is a constant, ℓ is also a constant. It is therefore equivalent to minimise with respect to $\eta = r_0/\ell$ or with respect to r_0. To do so, we need the derivative

$$\frac{\mathrm{d}\zeta}{\mathrm{d}\eta} = 1 - \frac{\zeta}{\eta} + \zeta^2, \tag{25}$$

which can be derived as follows: We have

$$\frac{\mathrm{d}\zeta}{\mathrm{d}\eta} = \frac{\mathrm{d}}{\mathrm{d}\eta}\left(\frac{J_1(\eta)}{J_0(\eta)}\right) = \frac{J_1'(\eta)}{J_0(\eta)} - \frac{J_1(\eta)J_0'(\eta)}{J_0^2(\eta)} = \frac{J_0(\eta) - \frac{1}{\eta}J_1(\eta)}{J_0(\eta)} + \frac{J_1^2(\eta)}{J_0^2(\eta)};$$

for the expressions of the derivatives of the Bessel functions, see Abramowicz and Stegun (1970). Then, we replace $J_1(\eta)/J_0(\eta)$ by ζ in this equation.

The energy can now be written as

$$\mathcal{E}_\ell = \frac{\Phi^2}{8\pi\ell}\left(-\frac{D}{b}\right),$$

and the minimisation yields[2]

$$\left.\frac{\mathrm{d}\mathcal{E}_\ell}{\mathrm{d}\eta}\right|_{r_0} = 0 = \frac{\Phi^2}{8\pi\ell}\left.\frac{\mathrm{d}}{\mathrm{d}\eta}\left(-\frac{D}{b}\right)\right|_{r_0} = \frac{\Phi^2}{8\pi b\ell}\left\{\zeta + 3\zeta^{-1} - 2\eta\zeta^{-1}\left(\zeta + \zeta^{-1}\right)\right\}. \tag{26}$$

The derivation of this equation is made easier by using the relations

$$b = 2\pi\eta\zeta\ell, \qquad \frac{\mathrm{d}\zeta}{\mathrm{d}\eta} = -D\frac{\zeta}{\eta}, \qquad \frac{\mathrm{d}(\eta\zeta)}{\mathrm{d}\eta} = \eta\zeta\left(\zeta + \zeta^{-1}\right),$$
$$\frac{\mathrm{d}D}{\mathrm{d}\eta} = -\left(\zeta + \zeta^{-1}\right) + \left(\zeta - \zeta^{-1}\right)D.$$

Note that b is not a constant in the energy minimisation. $\mathbf{A}_\mathrm{o}$ is not fixed by Φ alone. The subscript ℓ in $\mathcal{E}_\ell$ indicates that ℓ is kept constant in the energy minimisation.

The critical points are given by the intersections of

$$\eta = \frac{\zeta}{2} + \frac{\zeta}{1+\zeta^2} \tag{27}$$

(which stems from Equation (26)) and $\zeta = J_1(\eta)/J_0(\eta)$ (the boundary conditions), see Figure 1 and Table 1. The line energy is

$$\mathcal{E}_\ell|_{r_0} = \frac{\Phi^2}{(2\pi r_0)^2}\frac{3+\zeta^2}{16} = \frac{B^2b^2}{16\pi^2}\frac{(1+\zeta^2)^2}{\zeta^2(3+\zeta^2)}. \tag{28}$$

The critical points (see Figure 1) are the same as those obtained in KR (their Section 5), who also investigated a tube embedded in a pure vector potential, but in the limit of a tube

[2]We denote any quantity f evaluated at a critical point as $f|_{r_0}$. For example, $\frac{\partial D}{\partial \eta}|_{r_0} = 0$.

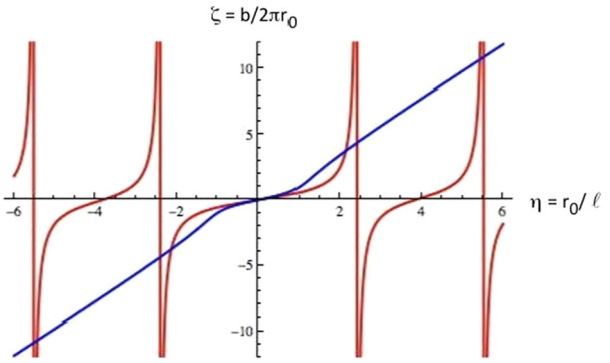

Figure 1 Red curve: $\zeta = J_1(\eta)/J_0(\eta)$ (the boundary condition), blue curve: $\partial\mathcal{E}/\partial r_0 = 0$. There is no magnetic field outside the rope. The critical points are the intersections of the red curves (asymptotes excluded) and the blue curves. We display the two first solutions for $\ell > 0$ and $\ell < 0$, corresponding to $b > 0$ (right-handed magnetic field lines of force) and $b < 0$ (left-handed lines of force). See Table 1 for numerical values. Adapted from Kleman and Robbins (2014).

Table 1 The first column is the label of the *stratum*, whose quantum number is given in the second and (equivalently) in the third column. The fourth column is $(\eta_J \zeta_J)^{-1}$. The fifth column is the line energy, to a factor $\Phi^2/(2\pi r_0)^2$. The sixth is the line energy, to a factor $B^2b^2/16\pi^2 = (\mathcal{I}/c)^2$, which tends very quickly to a maximum $\beta = 1$ when J increases. Adapted from Kleman and Robbins (2014).

J	$\eta_J = \frac{r_{0,J}}{\ell_J}$	$\zeta_j = \frac{b_J}{2\pi r_{0,J}}$	$\frac{2\pi\ell_J}{b_J}$	$\alpha = \frac{3+\zeta_J^2}{16}$	$\beta = \frac{(1+\zeta_J^2)^2}{\zeta_J^2(3+\zeta_J^2)}$
1	2.1288	3.7610	0.1249	1.07157	0.945798
2	5.4258	10.6657	0.0173	7.2973	0.991511
3	8.5950	17.0733	0.0068	18.4061	0.996616
4	11.7488	23.4123	0.0036	34.4460	0.998189
5	14.8973	29.7273	0.0023	55.4195	0.998874
10	30.6183	61.2039	0.00053	234.307	0.999733
100	313.3727	626.7421	4.0916×10^{-6}	24550.5	0.999997

embedded in a vanishing irrotational magnetic field, *i.e.*, the topological constant is an electric current, not a flux. The energy is the same (Equation (35) in KR is easily identified with Equation (28)). As shown there, the critical points are stable.

Figure 1 and Table 1 exhibit a splitting of the states into *strata* of quantum numbers ηs or, equivalently, ζs. These *strata* shall be assigned an integer from $J = 1$ for $\eta = 2.1288$ to $J = \infty$.

3.2. Merging of Flux Ropes

Flux rope reconnection is responsible for energy release in large amounts, see *e.g.*, Priest and Forbes (2000) for a review, and Linton (2006) for numerical calculations. From a global theoretical point of view, the merging of two ropes $[\Phi_1]$, $[\Phi_2]$ should yield, if it occurs, a rope $[\Phi = \Phi_1 + \Phi_2]$, independently of the mechanism by which this merging occurs; reciprocally, a rope $[\Phi]$ could split, if the event is energetically favoured, into $[\Phi_i]$ ropes, with $\Phi = \sum_i \Phi_i$. Note that the invariance of the current $[\mathcal{I}_i]$ (equivalently, of ℓ), employed

to calculate the *stratum* quantisation, does not mean that the currents obey a conservation law of the same type as the fluxes: the currents are not topological constants.

There is another conservation law, however, the conservation of the *magnetic helicity* [$\mathcal{H}_{\rm tot} = \iiint_V \mathbf{A}\cdot\mathbf{B}\,\mathrm{d}V$] (Berger and Field, 1984), which is often invoked. This law reads

$$\mathcal{H}_{\rm tot} = \sum_i \mathcal{H}_{i,\rm tot}, \qquad \mathcal{H}_{i,\rm tot} = \iiint_{V_i} \mathbf{A}\cdot\mathbf{B}\,\mathrm{d}V,$$

where each volume of integration is bordered by surfaces to which the magnetic field is tangent, $\mathbf{B}\cdot\mathbf{n} = 0$ (magnetic surfaces).

This law cannot be applied under this form to the merging (or splitting) of flux tubes because such a process cannot propagate instantaneously along the full length of the tubes even if the tubes are parallel all along; thus, the initial domain of merging (or splitting) necessarily involves a finite volume of a tube that is *not* bound by a magnetic surface. This is the magnetic helicity defined in Berger and Field (1984) relative to a local volume (which generally is not bordered by a magnetic surface), for which the conservation law still holds in ideal MHD and to a high approximation when the magnetic Reynolds number is large. In the straight tube case, this *relative magnetic helicity* takes the form $\mathcal{H}_R = 4\pi\int A_\theta B_\theta r\,\mathrm{d}r$ per unit length of the tube, which can be written, in the LFFF case under investigation, as

$$\mathcal{H}_R = 4\pi\ell^3 B^2 \frac{1}{J_0^2(\eta)}\int_0^\eta J_1^2(\rho)\rho\,\mathrm{d}\rho = 8\pi\ell\mathcal{E}\frac{\zeta^2-1}{\zeta^2+1}. \tag{29}$$

This expression derives from the relations already introduced, $\zeta = J_1(\eta)/J_0(\eta)$ and Equation (28), and the identity[3]

$$\int_0^\eta J_1^2(\rho)\rho\,\mathrm{d}\rho = \frac{1}{2}\eta^2\left\{J_0^2(\eta) + J_1^2(\eta) - 2\frac{J_0(\eta)J_1(\eta)}{\eta}\right\}.$$

Consider a collection of n identical parallel flux ropes, each defined by the parameters $\Phi = Bb\ell$, η, r_0 and a total energy $\mathcal{E} \propto n\Phi^2\alpha/r_0^2$, where $\alpha = (3+\zeta^2)/16$ (fifth column in Table 1). These flux ropes all belong to some *stratum* $\jmath$, which label we do not write explicitly. Assume that this collection merges to a unique flux rope $\Phi_k = B_k b_k \ell_k$, η_k, $r_{0,k}$, $\mathcal{E}_k \propto \Phi_k^2\alpha_k/r_{0,k}^2$. The relations that express the conservation of the relative magnetic helicity and of the flux are

$$\text{a)}\quad \ell\mathcal{E}\frac{\zeta^2-1}{\zeta^2+1} = \ell_k\mathcal{E}_k\frac{\zeta_k^2-1}{\zeta_k^2+1}, \qquad \text{b)}\quad n\Phi = \Phi_k. \tag{30}$$

In the calculations that follow, we use the relations and notations

$$r_0 \equiv \ell\eta, \qquad b \equiv 2\pi\ell\eta\zeta, \qquad \alpha = \frac{3+\zeta^2}{16}, \qquad \beta = \frac{(1+\zeta^2)^2}{\zeta^2(3+\zeta^2)}, \qquad u = \frac{\zeta^2-1}{\zeta^2+1},$$

where $\beta = \alpha/\eta^2$ is the energy expressed in units of $B^2b^2/(16\pi^2)$ (sixth column in Table 1). With these modifications, the energies can be written $\mathcal{E} = n(\Phi^2/\ell^2)\beta$, and $\mathcal{E}_k = n^2(\Phi^2/\ell_k^2)\beta_k$.

[3] Use in sequence Equation 11.3.31 ($\mu = -\nu = 1$) and Equation 9.1.27 ($\nu = 1$) from Abramowicz and Stegun (1970).

Using Equation (30)a, this yields

$$\frac{\mathcal{E}}{\mathcal{E}_k} = \frac{\ell_k}{\ell}\frac{u_k}{u}. \tag{31}$$

In addition, because $\mathcal{E} = n(\Phi^2/\ell^2)\beta$, $\mathcal{E}_k = n^2(\Phi^2/\ell_k^2)\beta_k$, we have

$$\frac{\mathcal{E}}{\mathcal{E}_k} \equiv \frac{1}{n}\left(\frac{\ell_k}{\ell}\right)^2 \frac{\beta}{\beta_k}. \tag{32}$$

Comparing these two expressions of the ratio $\mathcal{E}/\mathcal{E}_k$ yields

$$\frac{\ell_k}{\ell} = n\frac{\beta_k}{\beta}\frac{u_k}{u}, \tag{33}$$

and eventually,

$$\frac{\mathcal{E}}{\mathcal{E}_k} = n\frac{\beta_k}{\beta}\left\{\frac{u_k}{u}\right\}^2. \tag{34}$$

The energy variation

$$\triangle\mathcal{E} = \mathcal{E} - \mathcal{E}_k = \frac{n - \frac{\beta_k u_k^2}{\beta u^2}}{n}\mathcal{E} \tag{35}$$

is positive, $\triangle\mathcal{E} > 0$ implies

$$n - \frac{\beta_k u_k^2}{\beta u^2} > 0, \tag{36}$$

which is always satisfied as soon as $n \geq 1$ and $k < \jmath$, see Table 1. Thus, the merging of identical flux ropes is always favoured and yields a strong release of energy, as we show below.

Here are some numerical values of the quantity βu^2:

$$\beta_1 {u_1}^2 = 0.712495, \qquad \beta_2 {u_2}^2 = 0.957251,$$
$$\beta_5 {u_5}^2 = 0.994362, \qquad \beta_{10} {u_{10}}^2 = 0.998666.$$

These values are not very different from unity and tend very quickly to unity when the label of the *stratum* increases. However, in the first *stratum*, βu^2 is strongly separated from the higher *strata*. The energy release does not depend much on the value of k compared to the value $\jmath$ of the *stratum* of the original tubes; it is lower than $(1 - 1/n)\mathcal{E}$ if $k > \jmath$, higher otherwise, *cf.* Equation (35). We consider now some examples.

- If $n = 1$ *i.e.*, a unique original rope with $\jmath > 1$, it is evident that there is some release of energy if this tube transforms to a rope with $k < \jmath$. The strongest possible release of energy is when $k = 1$; thus, individual ropes relax to their lowest energy state, in the first *stratum* $k = 1$.
- If the original ropes are identical and belong to the first *stratum*, they merge into a unique rope belonging to the same *stratum*. From Equations (31) to (35), this yields with $\beta_k = \beta = \beta_1$, $u_k = u = u_1$

$$\frac{\mathcal{E}}{\mathcal{E}_1} = n, \qquad \triangle\mathcal{E} = \mathcal{E} - \mathcal{E}_1 = \frac{n-1}{n}\mathcal{E}. \tag{37}$$

The released energy is of the order of the energy of the original collection of ropes if n is large enough. Moreover, by using Equation (30)b and Equation (33), this yields

$$\frac{\ell_1}{\ell} = n, \qquad \frac{B_1 b_1}{Bb} = 1, \qquad \frac{b_1}{b} = n, \qquad \frac{r_{0,1}}{r_0} = n, \qquad \frac{B}{B_1} = n. \tag{38}$$

According to KR, $-2\pi\ell$ is the pitch of the vector field $\boldsymbol{v}$ ($\mathbf{B} = B\boldsymbol{v}$) and thus measures the inverse twist in a direction orthogonal to the tube axis; the corresponding number of pitches $r_0/|2\pi\ell|$ does not vary in the merging process when the same *stratum* is involved for the original tubes and the final tube, Equation (38). This pitch expands continuously, and the period b along the axis expands in the same proportion. In a sense, therefore, the topology of the flux lines has not been modified.

4. The Gold–Hoyle NLFFF Model in the A-Singularity Framework

This is a rather simple nonlinear force-free model (Gold and Hoyle, 1960), in which field lines are uniformly twisted in the direction of the axis; it was developed with the purpose of explaining solar flares. This model has been used in the numerical investigation of the reconnection of tubes (Linton, 2006), or the analysis of observations of interplanetary magnetic clouds, see examples below.

4.1. The Gold–Hoyle Model: A Reminder

The field inside the tube depends on three independent parameters, the flux Φ, the radius r_0 of the tube, and ϖ; the number of turns per unit length of a line of force is ϖ/q, where $q = 4\pi^2 r_0^2 \varpi^2$. So each line of force has the same pitch $b = q/\varpi$; this is the main property of the Gold–Hoyle (GH) model, which can be written $\cot\phi = 2\pi\varpi r$, where ϕ is the angle of the lines of force with a plane $z =$ constant. Note that $-2\pi\ell$ is the pitch along a radial line, which is a constant in the LFFF case. In the NLFFF case this is no longer true, ℓ is a function of r. Assuming $\mathbf{B}_\mathrm{o} = 0$, this means that:

a) *outside*

$$\mathbf{A}_\mathrm{o} = \left\{0, \frac{\Phi}{2\pi r}, -\Phi\varpi\right\}, \tag{39}$$

b) *inside*

$$\mathbf{B} = \left\{0, A\frac{2\pi\varpi r}{D_e}, A\frac{1}{D_e}\right\}, \qquad \mathbf{A}_\mathrm{i} = \left\{0, \frac{\Phi}{2\pi r}\frac{\ln D_e}{\ln(1+q)}, -\Phi\varpi\frac{\ln D_e}{\ln(1+q)}\right\}, \tag{40}$$

where

$$A = \Phi\frac{q}{\pi r_0^2 \ln(1+q)}, \qquad D_e = 1 + 4\pi^2\varpi^2 r^2, \qquad 4\pi^2\varpi^2 r_0^2 = q.$$

The energy is

$$\mathcal{E} = \frac{1}{2}\Phi^2\varpi^2\frac{1}{\ln(1+q)}. \tag{41}$$

The Beltrami parameter [$\alpha = 1/\ell$], which depends on r, is

$$\alpha = \frac{4\pi\varpi}{D_e}. \tag{42}$$

Let us denote

$$b_{\rm o} = -\frac{1}{\varpi}, \qquad b = \frac{q}{\varpi}, \qquad B = B_z(r_0) = \frac{A}{1+q},$$

$b_{\rm o}$ is the pitch of the helicoids $[\psi_{\rm o} = (b_{\rm o}/2\pi)\theta + z]$ orthogonal to the vector potential $\mathbf{A}_{\rm o}$. Because $\mathbf{A}_{\rm i} \cdot \mathbf{B}_{\rm i} = 0$, $b = q/\varpi$ is the pitch of the lines of force of $\mathbf{B}$ along the tube axis; it does not depend on the chosen line of force. It can be verified that $\int\int_0^{r_0} \nabla \times \mathbf{B}|_z r \mathrm{d}r\, \mathrm{d}\theta = Bb$; thus, the current takes the same expression as in the LFFF case, namely $\mathcal{I} = \frac{c}{4\pi} Bb$.

Finally, in analogy with the LFFF case, $\Phi = Bb\ell_{\rm GH}$, which makes it easy to check that

$$\ell_{\rm GH} = \frac{(1+q)\ln(1+q)}{4\pi\varpi q}.$$

This constant is related to the Beltrami parameter $1/\alpha(r_0) = (1+q)/(4\pi\varpi)$.

The relative magnetic helicity per unit length $\mathcal{H}_{\rm rel} = 4\pi \int\int A_{{\rm i},\theta} B_{{\rm i},\theta} r\, \mathrm{d}r\, \mathrm{d}\theta$ (Berger and Field, 1984) is

$$\mathcal{H}_R = \varpi \Phi^2. \tag{43}$$

4.2. Stable Critical Points

As above, we assume that the current $[\mathcal{I} \propto Bb]$ is a constant. This reads $\ell_{\rm GH} = $ constant, *i.e.*, employing $\mathrm{d}\ell_{\rm GH}/\mathrm{d}q = 0$,

$$\frac{\mathrm{d}\varpi}{\mathrm{d}q} \frac{(1+q)\ln(1+q)}{q\varpi} = \frac{1}{q^2}\big\{q - \ln(1+q)\big\}.$$

The critical points are given by $\partial\mathcal{E}/\partial q = 0$, namely

$$\frac{\partial \mathcal{E}}{\partial q} = \frac{1}{2}\Phi^2 \frac{\varpi^2}{q(1+q)\ln^2(1+q)}\big\{q - 2\ln(1+q)\big\}. \tag{44}$$

This expression vanishes for

$$q = 2.5128624\ldots. \tag{45}$$

The second derivative, calculated at this critical point,

$$\left.\frac{\partial^2 \mathcal{E}}{\partial q^2}\right|_{r_0} = \frac{1}{2}\Phi^2 \frac{\varpi^2}{q(1+q)\ln^2(1+q)} \frac{q-1}{q+1},$$

is positive; the configuration is stable. Because $\cot\phi(a) = q^{\frac{1}{2}}$, this yields an angle of $\phi(a) = 32.2452°$, independent of the radius of the tube.

The energy at the critical point is

$$\mathcal{E}_{\rm GH}|_{r_0} = \frac{\Phi^2}{(2\pi r_0)^2}, \tag{46}$$

which is to be compared to the value reported in the fifth column in Table 1. In this column the first coefficient, the smallest one, is 1.07157, which is close to unity, and is definitely smaller than the coefficients of $\Phi^2/4\pi^2 r_0^2$ in all the other *strata*. At this point of advancement of the theory, we believe that the difference between 1 and 1.07157 is not significant.

4.3. Merging

We start from a collection of n identical flux ropes, characterised by Φ, r_0, of total energy

$$\mathcal{E} = n\frac{\Phi^2}{(2\pi r_0)^2} \propto n\frac{q}{b^2}.$$

Their merging yields a unique flux rope $[n\Phi, r_{0,k}]$, of energy

$$\mathcal{E}_k = n^2\frac{\Phi^2}{(2\pi r_{0,k})^2} \propto n^2\frac{q}{b_k^2}.$$

Thus,

$$\frac{\mathcal{E}}{\mathcal{E}_k} = \frac{1}{n}\left(\frac{b_k}{b}\right)^2. \tag{47}$$

The conservation of the magnetic helicity yields $b_k = nb$. Thus, eventually

$$\frac{r_{0,k}}{r_0} = \frac{b_k}{b} = \frac{B}{B_k} = n, \qquad \frac{\mathcal{E}}{\mathcal{E}_k} = n, \tag{48}$$

where $B = A/D_e(r_0)$.

These results are similar to those obtained in the LFFF case, Equation (38).

5. Discussion

5.1. An Extended Summary of This Article

We have dwelt essentially upon the theoretical properties we expect for the Lundquist and Gold–Hoyle flux ropes, in the framework of a singularity model inspired in part by the theory of *defects* in condensed-matter physics (CMP). An important concept borrowed from CMP is that of the *topological constant*, which is in our case either the current $[\mathcal{I}]$ flowing through the tube or the magnetic flux Φ it carries. In the first case the topological constant is related to a singularity of an outer irrotational magnetic field $[\mathbf{B}_o]$ ($\frac{4\pi}{c}\mathcal{I} = \oint_C \mathbf{B}_o \cdot \mathrm{d}\mathbf{s}$), in the second case to a singularity of an outer irrotational vector potential $[\mathbf{A}_o]$ ($\Phi = \oint_C \mathbf{A}_o \cdot \mathrm{d}\mathbf{s}$), $[C]$ any loop surrounding the flux tube, the *core* of the singularity in CMP parlance. The topological constant is accompanied by another, *non-topological*, constant: Φ if the topological constant is $\mathcal{I}$, $\mathcal{I}$ if the topological constant is Φ. This article is about the Φ topological constant.

The field configurations of the singularity cores (the flux ropes themselves) are not different from those directly obtained without reference to their singular origin, incidentally, the flux ropes do not have to be singular, they are extended modes of the original singularities, but because of this origin, they can be classified into *quantised strata*. Each *stratum* is defined by either of two quantum numbers. In the LFFF case the scalars $\eta = r_0/\ell$ and $\zeta = b/(2\pi r_0)$, where r_0 is the radius of the rope, ℓ the Beltrami constant, b the pitch or the period along the tube axis (the inverse of the twist). In the GH NLFFF case there is only one *stratum*. In each *stratum* the parameters defining the flux rope (r_0, ℓ, b, B) can vary continuously, provided η or ζ are fixed. A remarkable fact is that the first *stratum* $\jmath = 1$ of the LFFF flux ropes (corresponding to the lowest energies) and the unique *stratum* of the NLFFF flux

ropes are defined by quantum numbers that are numerically very close. The analysis in Section 5.3 below, which compares the data inferred from observations to our theory, results in a strong feeling that all those data belong either to the LFFF first *stratum* or to the unique NLFFF *stratum*. This is what the theory would indeed suggest. Refined measurements, in particular of ζ, should mark the difference between the LFFF and the NLFFF approaches.

A well-known property used in the analysis of reconnection is that the *magnetic helicity* (under the relative form of Berger and Field (1984)) is conserved.[4] We show that the merging of equivalent ropes releases a large amount of energy. This merging brings the equivalent interacting ropes to a unique rope belonging to the first *stratum*.

5.2. Flux Ropes Are Singularities

It is a rather remarkable fact that the observation of flux tubes indicates that the magnetic flux lines are twisted, hence their denomination as *flux ropes*. Because of the boundary conditions, whatever they may be, the outer field (**B**, or **A**, or both) must also be twisted and, in the assumption of irrotationality, their level sets must be helical (as in Equations (5), (10), (12)) and thus behave as $1/r$, consequently singular for $r = 0$. This is a very strong property of flux ropes, which is difficult to get rid of; it originates in their twisted character.

5.3. Comparison to Observations of Magnetic Clouds

In situ observations in the interplanetary space provide a number of data on flux ropes, including magnetic clouds. These data have been thoroughly analysed by several authors in the frameworks of various flux rope models (Lunquist, Gold–Hoyle, non-force-free models, *etc*); thus we have estimates of r_0, ℓ, B_i and magnetic helicities in these various models that we can compare to the present theory. Our discussion relies mostly on the data reported in Dasso, Mandrini, and Démoulin (2003), Dasso *et al.* (2005) and Lepping *et al.* (1997).

a) *LFFF*. We pick three cases from the references above, where the raw data are analysed in the framework of the Lundquist model:

- Lepping *et al.* (1997) described a flux rope observed by *Wind* on 18 October 1995 that was characterised by the values $B = 24.3$ nT, $r_0 = 0.135$ AU, $\alpha = 1/\ell = 20$ AU^{-1}. These data yield $\eta = r_0/\ell \approx 2.7$.
- Dasso, Mandrini, and Démoulin (2003) reported the data collected for a hot tube observed by *Wind* on October 24–25 1995 as follows: $B = 7.2$ nT, $r_0 = 0.035$ AU, $\alpha = 1/\ell = 65.8$ AU^{-1}. These data yield $\eta \approx 2.303$.
- The 'small' magnetic clouds reported in Lepping *et al.* (1997) yield B in the range 13.8–15.9 nT, $r_0 \approx 1.6 \times 10^{-2}$ AU, $\alpha = 1/\ell$ in the range 100–170 AU^{-1}. Thus the value of η lies between 1.63 and 2.72.

All these values of the non-dimensional parameter η are quite close to η_1, Table 1, and in any case closer to η_1 than to η_2. This is all the more remarkable because the dispersion in the data (r_0, ℓ) deduced from the observations is rather large. Note also that there seems to be no correlation between the values of the magnetic field B_i and those of r_0.

Thus, if one adopts the value $\eta = \eta_1 = 2.1288$ as a best fit, then $\zeta = 3.7610$, $b = 2\pi r_0 = 0.827$ AU for *e.g.* $r_0 = 0.035$ AU, *etc*. Let us keep $r_0 = 0.035$ AU, then, other quantities

[4] We give in Equation (29) a closed expression of the relative helicity for a cylindrical tube, which is made possible by its quantised *stratum* character.

can be calculated, as the *energy per unit length* $\mathcal{E}|_{r_0}$ Equation (28), which amounts to $\mathcal{E}|_{r_0} = 0.518 \times 10^4$ J/m, or the *current* $\mathcal{I} = (c/4\pi)Bb = 2.1323 \times 10^{10}$ SI units, *i.e.* a current density $j_z = \mathcal{I}/\pi r_0^2 = 0.2462$ nT/s ($\pi r_0^2 = 8.66 \times 10^{19}$ m^2).

b) *NLFFF*. The raw data were analysed in the framework of the Gold–Hoyle model (Dasso, Mandrini, and Démoulin, 2003) for the *Wind* event on October 24 – 25 1995. This yields $r_0 = 0.035$ AU, $2\pi\varpi = 46.2$ AU^{-1}, thus $q = 2.6147$, which is remarkably close to our theoretical value $q = 2.5129$, Equation (45).

This discussion can be extended to the value of the current density j_z. With $q = 2.5129$ (the theoretical value) as above and taking for the other quantities the values from the data analysis, one derives by employing the relation $(\pi r_0^2) j_z = (qc/4(1+q)\pi\varpi)B_z(0)$, $j_z = 0.0302$ nT/s, which is eight times lower than the value obtained for the same MC in the LFFF model (Dasso *et al.*, 2005).

It is worth comparing these calculated values to the value of j_z in the *third* model analysed in Dasso, Mandrini, and Démoulin (2003) (a non-force-free field model with constant current density) the only model that allows estimating j_z directly from the raw data. It appears that the favoured value is $j_z = 0.12$ nT/s, which is very different from our NLFFF calculation above; on the other hand, this estimate of j_z is closer to the prediction made from the LFFF model.

Acknowledgements I am indebted to J.M. Robbins for long-lasting fruitful exchanges on the space physics of electromagnetism. I thank P. Démoulin for pointing out to me the possible relevance of the flux tube singularity theory to magnetic clouds, and for useful correspondence. Both made relevant remarks on the text. I am grateful to J.-L. Le Mouël, who read the manuscript with the utmost care and with whom I have had fruitful discussions. I am also very grateful to the anonymous referee for very valuable remarks. This is IPGP contribution No. 3382.

References

Abramowicz, M., Stegun, I.A. (eds.): 1970, *Handbook of Mathematical Functions*, Dover, New York.

Berger, M.A., Field, G.B.: 1984, The topological properties of magnetic helicity. *J. Fluid Mech.* **147**, 133. DOI.

Cantarella, J., DeTurck, D., Gluck, H.: 2002, Vector calculus and the topology of domains in 3-space. *Am. Math. Mon.* **109**, 409. DOI.

Dasso, S., Mandrini, C.H., Démoulin, P.: 2003, The magnetic helicity of an interplanetary hot flux tube. In: Velli, M., Bruno, R., Malara, F. (eds.) *Proc. Tenth Int. Solar Wind Conf.* **679**, Am. Inst. of Phys., New York, 786.

Dasso, S., Mandrini, C.H., Démoulin, P., Luoni, M.L., Gulisano, A.M.: 2005, Large scale MHD properties of interplanetary magnetic clouds. *Adv. Space Res.* **35**, 711. DOI.

Démoulin, P.: 2014, Evolution of interplanetary coronal mass ejections and magnetic clouds in the heliosphere. In: Schmieder, B., Malherbe, J.M., Wu, S.T. (eds.) *Nature of Prominences and Their Role in Space Weather*, *IAU Symposium* **300**, 1.

Fan, Y.: 2009, Magnetic fields in the solar convection zone. *Living Rev. Solar Phys.* **6**, 4. DOI.

Georgoulis, M.K., Titov, V.S., Mikić, Z.: 2012, Non neutralized electric current patterns in solar active regions: Origin of the shear-generating Lorentz force. *Astrophys. J.* **761**, 61.

Gold, T., Hoyle, F.: 1960, On the origin of solar flares. *Mon. Not. Roy. Astron. Soc.* **120**, 89.

Griffiths, D.J.: 1999, *Introduction to Electrodynamics*, 3rd edn. Prentice Hall, New York.

Hood, A.W., Archontis, V., MacTaggart, D.: 2012, 3D MHD flux emergence experiments: Idealized models and coronal interactions. *Solar Phys.* **278**, 3. DOI.

Kleman, M., Friedel, J.: 2008, Disclinations, dislocations and continuous defects: A reappraisal. *Rev. Mod. Phys.* **80**, 61. DOI.

Kleman, M., Robbins, J.M.: 2014, Tubes of magnetic flux and electric current in space physics. *Solar Phys.* **289**, 1173. DOI.

Lepping, R.P., Burlaga, L.F., Szabo, A., Ogilvie, K.W., Mish, W.H., Vassiliadis, D., Lazarus, A.J., Steinberg, J.T., Farrugia, C.J., Janoo, L., Mariani, F.: 1997, The Wind magnetic cloud and events of October 18 – 20, 1995: Interplanetary properties and as triggers for geomagnetic activity. *J. Geophys. Res.* **102**, 14049. DOI.

Linton, M.G.: 2006, Reconnection of nonidentical flux tubes. *J. Geophys. Res.* **111**, A12S09. DOI.

Lundquist, S.: 1950, Magnetohydrostatic fields. *Ark. Fys.* **2**, 361.

MacTaggart, D., Haynes, A.L.: 2014, On magnetic reconnection and flux rope topology in solar flux emergence. *Mon. Not. Roy. Astron. Soc.* **438**, 1500. DOI.

Mahajan, S.M., Yoshida, Z.: 1998, Double curl Beltrami flow: Diamagnetic structures. *Phys. Rev. Lett.* **81**, 4863. DOI.

Melrose, D.B.: 1996, Reply to comments by E.N. Parker. *Astrophys. J.* **471**, 497.

Möstl, C., Farrugia, C.J., Biernat, H.K., Leitner, M., Kilpua, E.K.J., Galvin, A.B., Luhmann, J.G.: 2009, Optimized Grad–Shafranov reconstruction of a magnetic cloud using STEREO-*Wind* observations. *Solar Phys.* **256**, 427. DOI.

Parker, E.N.: 1979, *Cosmical Magnetic Fields*, Clarendon, Oxford, 208.

Parker, E.N.: 1996, Inferring mean electric currents in unresolved fibril magnetic fields. *Astrophys. J.* **471**, 485. DOI.

Parker, E.N.: 2004, Tangential discontinuities in untidy magnetic topology. *Phys. Plasmas* **11**, 2328.

Parker, E.N.: 2009, Solar magnetism: The state of our knowledge and ignorance. *Space Sci. Rev.* **144**, 15.

Patsourakos, S., Vourlidas, A., Stenborg, G.S.: 2013, Direct evidence for a fast coronal mass ejection driven by the prior formation and subsequent destabilization of a magnetic flux rope. *Astrophys. J.* **764**, 125. DOI.

Priest, E., Forbes, T.: 2000, *Magnetic Reconnection: MHD Theory and Applications*, Cambridge University Press, Cambridge.

Schmieder, B., Démoulin, P., Aulanier, G.: 2013, Solar filament eruptions and their physical role in triggering coronal mass ejections. *Adv. Space Res.* **51**, 1967. DOI.

Stenflo, J.O.: 1978, The measurement of solar magnetic fields. *Rep. Prog. Phys.* **41**, 865. DOI.

Török, T., Leake, J.E., Titov, V.S., Archontis, V., Mikić, Z., Linton, M.G., Dalmasse, K., Aulanier, G., Kliem, B.: 2014, Distribution of electric currents in solar active regions. *Astrophys. J. Lett.* **782**, L10. DOI.

Vourlidas, A.: 2014, The flux rope nature of coronal mass ejections. *Plasma Phys. Control. Fusion* **56**, 064001.